

## NMR determination of the B substitutional site in $UBe_{13-x}B_x$

E. T. Ahrens, P. C. Hammel, R. H. Heffner, A. P. Reyes, and J. L. Smith  
*Los Alamos National Laboratory, Los Alamos, New Mexico 87545*

W. G. Clark

*Department of Physics, University of California at Los Angeles, Los Angeles, California 90024*

(Received 17 March 1993)

We report  $^9\text{Be}$ ,  $^{10}\text{B}$ , and  $^{11}\text{B}$  NMR measurements in  $U(\text{Be},\text{B})_{13}$  which show an exclusive substitution site for the boron dopant into the  $m\bar{3}$  or cubic site of the  $UBe_{13}$  lattice.

### I. INTRODUCTION

Recently, there has been much interest in the effect of doping small amounts of boron into the unconventional heavy-fermion superconductor  $UBe_{13}$ .  $UBe_{13-x}B_x$  ( $x \sim 0.03$ ) has been shown to exhibit several remarkable properties.<sup>1-4</sup> The most striking is the large enhancement in the specific-heat discontinuity  $\Delta C$  at the superconducting transition temperature ( $T_c$ ).  $\Delta C$  shows a strong boron concentration dependence which reaches a maximum value for  $x \sim 0.03$ , nearly twice as large as in the pure compound. The effect of B doping on  $T_c$  is small,<sup>4</sup> which is in sharp contrast to what is observed when other nonmagnetic impurities are substituted for Be at comparable doping levels.<sup>5</sup> Also, there is evidence<sup>3,4</sup> for a systematic reduction in the energy scale associated with spin fluctuations as the B concentration is increased. It has been suggested that these observations provide evidence for a correlation between the superconducting coupling strength and the energy scale characterizing these spin fluctuations.<sup>3,4</sup>

The compound  $UBe_{13}$  crystallizes in the cubic  $\text{NaZn}_{13}$  structure<sup>6</sup> with eight formula units per unit cell. The space group is  $O_h^6-Fm\bar{3}c$ , with eight equivalent U in  $\pm(1/4, 1/4, 1/4)$ , and two nonequivalent Be sites: eight Be(I) in  $\pm(0, 0, 0)$ ,  $\pm(1/2, 1/2, 1/2)$  and 96 Be(II) at  $\pm(0, y, z)$ ,  $\pm(0, y, \bar{z})$ ,  $\pm(1/2, z, y)$ ,  $\pm(1/2, \bar{z}, y)$ , plus three-fold rotation and face centering equivalent positions. The values of  $y$  and  $z$  have been calculated to be 0.1761 and 0.1141, respectively. Of importance to our discussion is that Be(II) possesses cubic symmetry ( $m\bar{3}$ ), whereas the symmetry of Be(I) is lower ( $m$ ). The Be(I) is located at the center of an icosahedron formed by 12 nearest-neighbor Be(II) sites. This configuration is, surprisingly, isostructural to the nearest-neighbor configuration of hcp Be metal. The sublattice consisting of only U and Be(I) atoms forms a simple CsCl-type structure. Shown in Fig. 1 is a formula unit cell displaying both nonequivalent Be sites. The U site (not shown) is approximately located at the cube's center. The faces of the cube show the 24 nearest-neighbor Be(II) sites to U, which are located on the corners of a 38-sided polyhedron or snub cube.

Because of the similarity of ionic radii of  $\text{Be}^{2+}$  and  $\text{B}^{3+}$ , one expects that B will be substituted into a Be site.

There are, however, other possibilities for the B substitution. The phase diagrams for the U-B and B-Be systems show that it may be possible to precipitate a second phase instead of forming the compound  $UBe_{13-x}B_x$ . For example, unlike the U-Be system where  $UBe_{13}$  is the only stable compound, the U-B system can stabilize three compounds  $UB_2$ ,  $UB_4$ , and  $UB_{12}$ . Any of these compounds could be a potential second phase. Other possibilities for the B location include an interstitial lattice position other than a specific crystallographic site, or the deposition of elemental B in grain boundaries. Indirect evidence that the B is actually entering into the material and affecting the electronic properties can be seen in heat-capacity and resistivity measurements.<sup>1-4</sup> X-ray-diffraction experiments observe no detectable changes in lattice parameters despite the slightly smaller ionic radius of B. However, x-ray-scattering diffraction is limited in sensitivity because the amount of substituted B is extremely small and because of the difficulty in detecting the presence of light elements with a small x-ray-scattering cross section such as B.

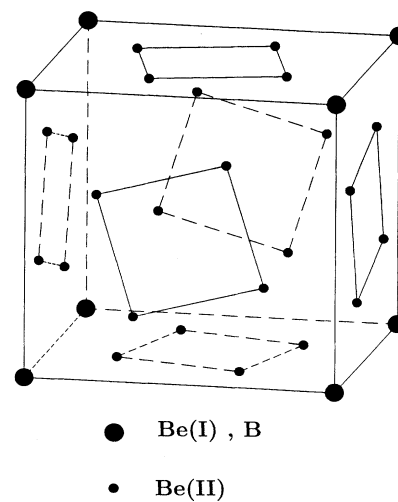


FIG. 1. One formula unit cell of  $UBe_{13}$  showing both nonequivalent Be sites and the B doping site. The U site is not shown and is located at approximately the cube's center.

A local probe such as NMR provides a powerful tool for elucidating impurity structures. Within a given sample of  $\text{UBe}_{13-x}\text{B}_x$  we are able to detect NMR resonances from three nuclei:  $^9\text{Be}$ ,  $^{11}\text{B}$ , and  $^{10}\text{B}$ . A simple analysis of the field-swept spectra for the three nuclei is presented which exploits the known quadrupolar interaction parameters established from detailed single-crystal studies [7] of pure  $\text{UBe}_{13}$ . The results indicate that the B is substituted exclusively into the cubic  $\text{Be}_1$  site. Measurements of the spin-lattice-relaxation rate ( $1/T_1$ ) of the B nuclei indicate that all the substituted B resides in a single phase of the sample and exhibits the characteristic enhancement of the density of states at the Fermi energy seen in pure  $\text{UBe}_{13}$  and many other heavy-fermion compounds.<sup>8</sup>

## II. EXPERIMENT

A number of compositions of polycrystalline  $\text{UBe}_{13-x}\text{B}_x$  were prepared using a standard arc-melting technique. The B concentrations studied were  $x=0.010$ ,  $0.030$ , and  $0.067$  from the same series of samples used in thermodynamic, transport, and  $\mu\text{SR}$  studies.<sup>2-4</sup> The NMR samples were prepared from portions of polycrystalline ingots which were powdered to particle sizes of diameter  $38 \leq d \leq 125 \mu\text{m}$ . Ten percent by volume of  $-325$  mesh,  $99.99\%$  Al was mixed in with the sample as a local-field reference for shift measurements. Approximately one gram of sample was used per B concentration. NMR spectra were obtained with a conventional pulsed NMR spectrometer by integrating the spin-echo intensity with a boxcar integrator while sweeping the applied magnetic field. The spin-lattice-relaxation rate was measured by integrating the spin-echo intensity at various times after a comb of saturating pulses. The time dependence of the recovery of the magnetization fit a single exponential.

In order to confirm that the boron concentration is approximately equal to the nominal values, we measured the relative number of  $^{11}\text{B}$  to  $^9\text{Be}$  nuclei in each sample using NMR. This was obtained from the ratio of the integrated areas under the field-swept spectra for  $^{11}\text{B}$  and  $^9\text{Be}$  within a given sample. These measurements were made at constant frequency and corrections were made for the relative sensitivity and  $T_2$  for the respective nuclei. The values obtained are in agreement with the nominal values to better than 35%. But more importantly, this measurement confirms that the B resonance we observe includes essentially all the boron in the sample.

## III. RESULTS AND DISCUSSION

Field-swept spectra for the  $^9\text{Be}$ ,  $^{11}\text{B}$ ,  $^{10}\text{B}$ , and  $^{27}\text{Al}$  nuclei in the  $x=0.030$  sample are shown in Fig. 2. The field axis for each spectrum taken at various spectrometer frequencies is normalized to the centroid of each resonance, except for the  $^9\text{Be}$  spectrum which is normalized to the approximate position of the Be(I) feature. In Fig. 3 we plot the field dependence of the linewidths of the  $^{11}\text{B}$ ,  $^{10}\text{B}$ , and  $^{27}\text{Al}$  nuclei, obtained from the full width at half maximum (FWHM) for a Gaussian fit.

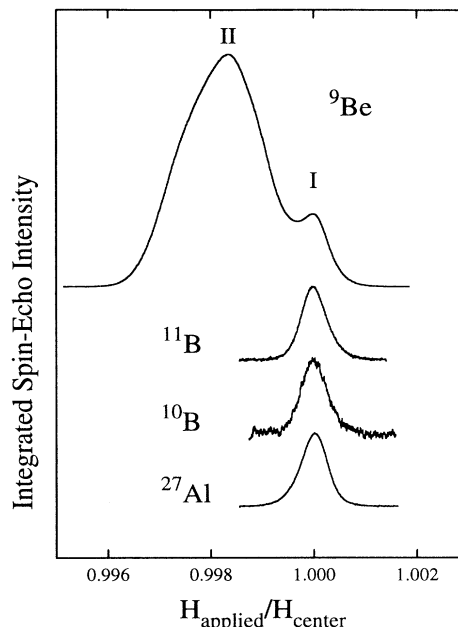


FIG. 2. Field-swept spectra taken at 4 K for the  $^9\text{Be}$ ,  $^{11}\text{B}$ ,  $^{10}\text{B}$ , and  $^{27}\text{Al}$  in the  $x=0.030$  sample. The field axes are normalized to the center of each resonance, except for the  $^9\text{Be}$  spectrum which is normalized to the approximate position of the Be(I) feature (labeled). Note the absence of a Be(II) feature in the B resonances and the comparable widths and line shapes of  $^{11}\text{B}$ ,  $^{10}\text{B}$ , and  $^{27}\text{Al}$ . The spectra taken at spectrometer frequencies of 52 MHz for  $^9\text{Be}$  and  $^{10}\text{B}$ , and 95 and 63 MHz for  $^{11}\text{B}$  and  $^{27}\text{Al}$ , respectively.

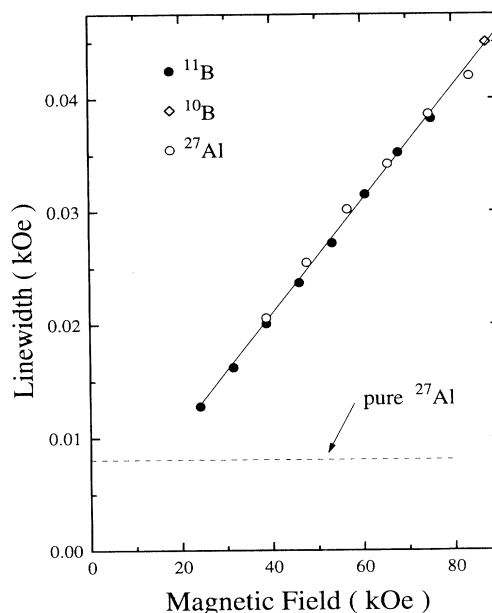


FIG. 3. Magnetic-field dependence of the linewidth for  $^{11}\text{B}$ ,  $^{10}\text{B}$ , and  $^{27}\text{Al}$ , measured from the FWHM for a Gaussian fit. All linewidths follow the same linear field dependence resulting from the large  $\chi_V$  of the powdered sample. The approximately field-independent linewidth of pure Al is also shown for comparison.

The  $^9\text{Be}$  spectrum shows two features comprising both nonequivalent Be sites. The low symmetry of the Be(II) site gives rise to a quadrupolar interaction of strength,<sup>7</sup>

$$v_Q = 3e^2Qq/2I(I-1)h = 328 \text{ kHz}, \quad (1)$$

where  $eq$  is the strength of the electric-field gradient (EFG),  $Q$  is the value of the quadrupole moment, and  $I=3/2$  is the nuclear spin for  $^9\text{Be}$ . This is convoluted with a small anisotropic Knight shift and magnetic broadening, forming a broad powder pattern. The cubic symmetry of the Be(I) site means that both the EFG and the anisotropic Knight shift are zero. This site contributes one-thirteenth of the total spectral weight and exhibits a symmetric line shape which partially overlaps the Be(II) line. The  $^{11}\text{B}$  and  $^{10}\text{B}$  nuclei have spin  $I=3/2$  and  $I=3$  and a natural abundance of 80.2 and 19.8%, respectively. The spectra of both nuclei exhibit a single, approximately Gaussian line shape. In order to analyze the B spectra, we start by considering the expected quadrupolar split powder pattern for B randomly substituted into both Be sites. We will assume that the EFG at a boron impurity in a Be(II) site is equal to the value measured in pure  $\text{UBe}_{13}$ . In general, however, one expects a modification to the electronic contribution to the EFG as a result of the substitution of trivalent  $\text{B}^{3+}$  for divalent  $\text{Be}^{2+}$ . This originates from at least two sources. First, there is an additional local electronic contribution to the EFG due to the necessity for additional conduction-electron screening of the excess charge, which generally results in a small enhancement of the strength of the EFG [9]. Second, there is a difference in the Sternheimer antishielding factor between  $\text{Be}^{3+}$  and  $\text{Be}^{2+}$ . This is a small effect, however, because the two ions have identical core electron configurations. One can estimate the hypothetical "width" of a Be(II) feature in a  $^{11}\text{B}$  spectrum from the magnitude of  $v_Q(^{11}\text{B})$ . This is a measure of the splitting between quadrupolar satellites and approximates the width of the resulting quadrupolar powder pattern. The value of the quadrupole moment  $Q$  of  $^{11}\text{B}$  is 80% of that of Be, which gives  $v_Q(^{11}\text{B}) \sim 262$  kHz. This yields a line of width  $\sim 192$  Oe, several times the observed  $^{11}\text{B}$  linewidth within the measured field range (Fig. 3). For a random substitution of B into both Be sites, the  $^{11}\text{B}$  spectrum would have the same two features as the Be spectrum, except for a slightly smaller overall width at a constant field. The  $^{10}\text{B}$  has  $I=3$  and a value of  $Q$  that is 60% greater than Be. Expression (1) gives  $v_Q(^{10}\text{B}) \sim 131$  kHz and a splitting between only the inner pair of the six satellites of  $\sim 287$  Oe, again much greater than the observed linewidth (Fig. 3). The observation of a single line for both B spectra and the absence of quadrupolar broadening is explained if the boron is located at a point of cubic symmetry where the EFG is zero.

Next we consider the effect of an interstitial B substitution. This would create local disorder around the impurity site and thus a distribution in the local EFG. First-order quadrupolar interactions due to this distribution would have a different effect on the linewidths of half-integral and integral spin nuclei. For half-integral spin nuclei such as  $^{11}\text{B}$ , the effect is to broaden or make the satellites completely unobservable, but leave the width of

the central transition ( $m = \frac{1}{2} \leftrightarrow -\frac{1}{2}$ ) unaffected. In integral spin nuclei like  $^{10}\text{B}$ , the same EFG distribution would cause a broadening of all allowed transitions, making the overall linewidth broader than that of  $^{11}\text{B}$ . The observation of comparable linewidths for constant applied magnetic field for both  $^{11}\text{B}$  and  $^{10}\text{B}$  cannot be explained if a significant distribution in EFGs existed at the B substitution site, and thus an interstitial B substitution is unlikely.

The field dependence of the linewidth for the  $^{11}\text{B}$  nuclei was investigated in order to determine the origin of the width and to look for evidence of an anisotropic Knight shift. Figure 3 shows the  $^{11}\text{B}$  results for the  $x=0.030$  sample at  $T=4$  K. We also observe that the widths of the  $^{10}\text{B}$  and  $^{27}\text{Al}$  lines have identical field dependences and therefore the same broadening mechanism is dominant for all three nuclei. One expects bulk sample magnetic-field inhomogeneities to have an important contribution to the line shape because of the huge susceptibility of these materials.<sup>10</sup> Drain discusses two magnetic line broadening mechanisms for a paramagnetic sample of packed spheroids.<sup>11</sup> The first is due to the dipole fields from the surface magnetization of neighboring particle grains. This causes a symmetric broadening of roughly Gaussian line shape. The second interaction causes an asymmetric broadening due to variations in internal demagnetization fields within individual particles as a result of deviations from sphericity. Broadening due to the first mechanism has been estimated<sup>11</sup> assuming a cubic close-packed ensemble of spherical particles to be  $\Delta H \approx 3\chi_V H_0$  at the FWHM, where  $\chi_V$  is the volume susceptibility and  $H_0$  is the applied field. The slope of a least-squares fit through the linewidth data in Fig. 3 is  $5.01 \times 10^{-4}$  and is in good agreement with  $3\chi_V$ , where the measured bulk susceptibility is  $\chi_V = 1.64 \times 10^{-4}$  emu/cm<sup>3</sup> at 4 K. Thus, the Gaussian line shape and magnitude of the linewidth for the three nuclei can be explained by classical magnetic effects. These observations are quantitatively the same for the  $x=0.010$  and  $x=0.067$  samples.

The spin-lattice-relaxation rate ( $1/T_1$ ) is sensitive to the low-frequency fluctuation spectrum of electronic spin excitations in magnetic systems. In  $\text{UBe}_{13}$  and other heavy-fermion systems,  $1/T_1$  exhibits the same large enhancement at low temperatures in the low-frequency excitations that is responsible for the characteristically large electronic specific heat observed in these materials. We have measured  $1/T_1$  for the  $^{11}\text{B}$  nucleus in the  $x=0.030$  sample at 4 and 77 K and find  $1/T_1 = 2.78 \pm 0.03 \text{ sec}^{-1}$  and  $4.25 \pm 0.09 \text{ sec}^{-1}$ , respectively. For comparison, in pure  $\text{UBe}_{13}$ ,  $1/T_1$  of  $^9\text{Be}$  at 4 and 77 K is approximately 0.60 and  $0.96 \text{ sec}^{-1}$  respectively.<sup>12</sup> These values differ by less than a factor of 5 in magnitude compared to the borated sample and both show a similar behavior of the product  $1/T_1 T$ . Although little NMR data exist on semiconducting elemental B, the spin-lattice relaxation rate is quadrupolar in nature and the time dependence to the recovery of the magnetization exhibits multiexponential behavior<sup>13</sup> which is unlike our observed single exponential recovery.  $^{11}\text{B}$  NMR measurements in  $\text{UB}_2$ ,<sup>14</sup> a potential second phase, show a

Korringa-like behavior and give  $1/T_1 \cong 0.01 \text{ sec}^{-1}$  at 4 K, which is three orders of magnitude smaller than what we measure. These comparisons emphasize that the boron we observe probes the heavy-fermion enhancement and does not originate from elemental boron or from a second phase.

#### IV. CONCLUSION

We present strong evidence from NMR measurements that shows that the boron in  $\text{UBe}_{13-x}\text{B}_x$  is doped exclusively into the cubic Be(I) site.

#### ACKNOWLEDGMENTS

We thank W. P. Beyermann, Z. Fisk, D. E. MacLaughlin, and J. D. Thompson for useful discussions. One of us (E.T.A.) acknowledges the support of the University of California Institutional Collaborative Research (INCOR) program in high-temperature superconductivity and the Associated Western Universities (AWU). Work at Los Alamos was performed under the auspices of the U.S. Department of Energy.

- 
- <sup>1</sup>Z. Fisk and H. R. Ott, *Int. J. Mod. Phys. B* **3**, 535 (1989); E. Felder, A. Bernasconi, H. R. Ott, Z. Fisk, and J. L. Smith, *Physica C* **162-164**, 429 (1989).
- <sup>2</sup>W. P. Beyermann, R. H. Heffner, M. F. Hundley, J. D. Thompson, J. L. Smith, and Z. Fisk, *Bull. Am. Phys. Soc.* **36**, 764 (1991).
- <sup>3</sup>R. H. Heffner, W. P. Beyermann, M. F. Hundley, J. D. Thompson, J. L. Smith, Z. Fisk, K. Bedell, P. Birrer, C. Baines, F. N. Gygax, B. Hitti, El Lippelt, H. R. Ott, A. Schenck, and D. E. MacLaughlin, *J. Appl. Phys.* **69**, 5481 (1991).
- <sup>4</sup>W. P. Beyermann, R. H. Heffner, J. L. Smith, M. F. Hundley, P. C. Canfield, J. D. Thompson, and Z. Fisk (unpublished).
- <sup>5</sup>H. M. Mayer, U. Rauchschwalbe, F. Steglich, G. R. Stewart, and A. L. Giogi, *Z. Phys. B* **64**, 299 (1986).
- <sup>6</sup>D. P. Shoemaker, R. E. Marsh, F. J. Ewing, and L. Pauling, *Acta Crystallogr.* **5**, 637 (1952).
- <sup>7</sup>W. G. Clark, M. C. Lan, G. van Kalker, W. H. Wong, Cheng Tien, D. E. MacLaughlin, J. L. Smith, Z. Fisk, and H. R. Ott, *J. Magn. Magn. Mater.* **63-64**, 396 (1987).
- <sup>8</sup>See, for example, D. E. MacLaughlin, *J. Magn. Magn. Mater.* **47-48**, 121 (1985).
- <sup>9</sup>E. N. Kaufmann and R. J. Vianden, *Rev. Mod. Phys.* **51**, 161 (1979).
- <sup>10</sup>H. R. Ott and Z. Fisk, in *Handbook on the Physics and Chemistry of the Actinides*, edited by A. J. Freeman and G. H. Landers (Elsevier, Amsterdam, 1987).
- <sup>11</sup>L. E. Drain, *Proc. Phys. Soc. London* **80**, 1380 (1962).
- <sup>12</sup>W. G. Clark, Z. Fisk, K. Glover, M. D. Lan, D. E. MacLaughlin, J. L. Smith, and C. Tien, in *Proceedings of the Seventeenth International Conference on Low-Temperature Physics*, edited by U. Eckern, A. Schmid, W. Weber, and H. Wuhl (North-Holland, Amsterdam, 1984), p. 227.
- <sup>13</sup>T. V. Hynes and M. N. Alexander, *J. Chem. Phys.* **54**, 5296 (1971).
- <sup>14</sup>M. Kuznietz and J. J. Spokas, *Bull. Am Phys. Soc.* **15**, 274 (1970).